Water Research 221 (2022) 118832

Contents lists available at ScienceDirect

Water Research

journal homepage: www.elsevier.com/locate/watres

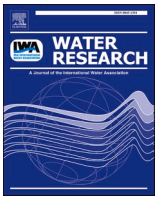

Exploring organic micropollutant biodegradation under dynamic substrate loading in rapid sand filters

Jinsong Wang [a], Baptiste A.J. Poursat [a], Jiahao Feng [a], David de Ridder [b], Chen Zhang [c], Albert van der Wal [a,b], Nora B. Sutton [a,*]

[a] Environmental Technology, Wageningen University & Research, P.O. Box 17, 6700 AA Wageningen, The Netherlands
[b] Evides Water Company N.V., Schaardijk 150, 3063 NH Rotterdam, The Netherlands
[c] Laboratory of Microbiology, Wageningen University & Research, P.O. Box 8033, 6700 EH Wageningen, The Netherlands

ARTICLE INFO

Keywords:
Micropollutant biodegradation
Dissolved organic matter
Ammonia
Substrate loading rate
Empty bed contact time
Rapid sand filter

ABSTRACT

Microbial removal of trace organic micropollutants (OMPs) from drinking water sources remains challenging. Nitrifying and heterotrophic bacteria in rapid sand filters (RSFs) are capable of biodegrading OMPs while growing on ammonia and dissolved organic matter (DOM). The loading patterns of ammonia and DOM may therefore affect microbial activities as well as OMP biodegradation. So far, there is very limited information on the effect of substrate loading on OMP biodegradation at environmentally relevant concentrations (~ 1 μg/L) in RSFs. We investigated the biodegradation rates of 16 OMPs at various substrate loading rates and/or empty bed contact times (EBCT). The presence of DOM improved the biodegradation of paracetamol (41.8%) by functioning as supplementary carbon source for the heterotrophic degrader, while hindering the biodegradation of 2,4-D, mecoprop and benzotriazole due to substrate competition. Lower loading ratios of DOM/benzotriazole benefited benzotriazole biodegradation by reducing substrate competition. Higher ammonia loading rates enhanced benzotriazole removal by stimulating nitrification-based co-metabolism. However, stimulating nitrification inhibited heterotrophic activity, which in turn inhibited the biodegradation of paracetamol, 2,4-D and mecoprop. A longer EBCT promoted metformin biodegradation as it is a slowly biodegradable compound, but suppressed the biodegradation of paracetamol and benzotriazole due to limited substrate supply. Therefore, the optimal substrate loading pattern is contingent on the type of OMP, which can be chosen based on the priority compounds in practice. The overall results contribute to understanding OMP biodegradation mechanisms at trace concentrations and offer a step towards enhancing microbial removal of OMPs from drinking water by optimally using RSFs.

1. Introduction

Organic micropollutants (OMPs), including pharmaceuticals (Phillips et al., 2015), pesticides (Björklund et al., 2011), and industrial compounds, are present at trace concentrations in surface water and groundwater (Schwarzenbach et al., 2006). Public concerns about the occurrences, ecotoxicities, and fates of OMPs in drinking water production are continuously rising due to their (potential) toxicity to both environmental and human health (Ben et al., 2018). Even though many techniques, such as activated carbon adsorption (Kim and Kang, 2008; Piai et al., 2019), advanced oxidation (Westerhoff et al., 2005; Ormad et al., 2008), ultraviolet irradiation (Yang et al., 2014) and membrane filtration (Košutić et al., 2005; Sarkar et al., 2007), effectively remove certain OMPs from drinking water, they share the disadvantages of high cost and high energy consumption (Košutić et al., 2005; Sarkar et al., 2007). An economically promising approach would be to remove OMPs using indigenous microbial communities in rapid sand filters (RSFs) (Hedegaard et al., 2014; Feld et al., 2016, 2018; Zhou et al., 2022), a widely installed facility at drinking water production plants (DWPPs) (Benner et al., 2013).

Various microbial communities that colonize sand granules as biofilm can facilitate the biological conversion of multiple substrates in RSFs (Hu et al., 2020). For instance, nitrifying bacteria catalyze the oxidation of ammonia (Lee et al., 2014; Fowler et al., 2018; Albers et al., 2018; Poghosyan et al., 2020), whereas heterotrophic bacteria can mineralize dissolved organic matters (DOM) (Bar-Zeev et al., 2012;

* Corresponding author.
E-mail address: nora.sutton@wur.nl (N.B. Sutton).

https://doi.org/10.1016/j.watres.2022.118832
Received 12 May 2022; Received in revised form 1 July 2022; Accepted 6 July 2022
Available online 7 July 2022

Terry and Summers, 2018; Hu et al., 2020). Both of them have been reported as OMP degraders (Benner et al., 2013; Wang et al., 2021). Nitrifying bacteria can biodegrade OMPs via co-metabolism (Fernandez-Fontaina et al., 2016; Trejo-Castillo et al., 2021; Wang et al., 2022). Rattier et al. (2014) reported that using a nitrification inhibitor limited or even stopped the removal of ketoprofen, gemfibrozil, furosemide, acetaminophen, caffeine and lincomycin, which confirmed the key role of nitrifying bacteria in OMP biodegradation. In addition, heterotrophic bacteria can biotransform OMPs or even mineralize them as energy sources (Elhadi et al., 2006; Hedegaard et al., 2014; Albers et al., 2015; Vandermaesen et al., 2016).

Due to their trace concentrations (several ng/L ~ μg/L) in drinking water sources, OMPs mainly serve as secondary substrates for microbial co-metabolisms (Stratton et al., 1983; Zearley and Summers, 2012), as the typical threshold concentrations for primary cellular bioprocesses are way higher (40–800 μg/L) (Stratton et al., 1983). Consequently, the availability of primary substrates (e.g., ammonia and DOM) may influence the degraders' activity and hence the OMP biodegradation (Maeng et al., 2011; Liu et al., 2014; Trejo-Castillo et al., 2021). Moreover, OMPs differ in their biodegradability resulting in different removal patterns for a mix of OMPs under stable substrate concentrations (He et al., 2018). However, little is known about the effects of availability of ammonia and DOM on the biodegradation of multiple OMPs, especially under RSFs-like hydraulic conditions. Interrogating the OMP biodegradation behaviors in an environment-realistic continuous mode will help to understand the effects of primary substrate availability on OMP biodegradation in field RSFs.

In RSFs, the loading rate of substrates determines their availability for microorganisms, which in turn influences the microbial activities. Lee et al. (2014) reported that the nitrification activity of RSFs was dictated by the ammonia loading rate rather than ammonia concentration or volumetric flow velocity individually. Loading rates of ammonia and DOM influence the activities of nitrifying and heterotrophic bacteria in RSFs and may therefore determine the biodegradation rates of OMPs. Yet, knowledge about the effects of primary substrate loading rates on OMP biodegradation rate is scarce. We hereby propose two hypotheses: (i) higher ammonia loading rates result in higher nitrification activity and may thereby enhance the autotrophic co-metabolism of OMPs; (ii) increasing the DOM loading rate on the one hand improves OMP biodegradation by enhancing the activity of the heterotrophic community, but on the other hand, reduces OMP biodegradation due to substrate competition.

With a fixed sand bed height, changing the volumetric flow velocity results in different empty bed contact times (EBCT). EBCT can critically affect OMP biodegradation (Paredes et al., 2016; Wang et al., 2021). Shorter EBCT could benefit the biodegradation of easily biodegradable compounds, as increased substrate loading rates support microbial activity and can compensate for lower contact time between OMPs and biofilms (Paredes et al., 2016); however, it may limit the degradation of slowly biodegradable compounds due to the reduction in contact time (Paredes et al., 2016). Thus, a prolonged EBCT might be advantageous for the biodegradation of slowly biodegradable OMPs, but negligibly or even negatively affects the elimination of readily biodegradable OMPs.

The aim of this research is to systematically investigate the effects of additional primary substrates, substrate loading rates and EBCTs on the biodegradation rates of a range of trace OMPs in RSFs. A mixture of sixteen OMPs, including nine pesticides, four pharmaceuticals and three industrial chemicals, was spiked at a concentration of approximately 1 μg/L in column-scale RSFs. Three columns were parallelly operated with different feeding strategies: without ammonia and DOM (control), only with DOM, and only with ammonia. By changing either the initial substrate concentrations or volumetric flow velocity, dynamic loading rates of ammonia, DOM and OMPs as well as EBCTs were applied in different operational phases. The OMP biodegradation kinetic of each phase was determined by pseudo-first-order kinetic models. The results expand our understanding of OMP biodegradation processes and offer insight into optimizing the operational conditions to improve biological removal of OMPs in RSFs.

2. Materials and methods

2.1. Organic micropollutants and dissolved organic matters

This study selected nine pesticides (2,6-dichlorobenzamide (BAM), mecoprop, 2,4-dichlorophenoxyacetic acid (2,4-D), chloridazon, methyl-desphenyl-chloridazon, desphenyl-chloridazon, bentazone, metolachlor and metribuzin), four pharmaceuticals (paracetamol, salicylic acid, caffeine, and metformin) and three industrial chemicals (perfluorooctanoic acid (PFOA), diglyme and benzotriazole) as target compounds. These compounds display a broad variety of physicochemical properties (Table S1); they have been observed in water sources for drinking water production in the Netherlands and are regarded as priority OMPs for removal. The commercial companies and stock preparation of OMPs are given in Text S1. The measured concentrations of all OMPs in spiked influent were around 800 ng/L, except for salicylic acid, which was at a median concentration of 76 ng/L (Fig. S1). Salicylic acid, as a readily biodegradable compound (Combarros et al., 2014; Hack et al., 2015), could have been biodegraded in the feeding tubes.

DOM were extracted from a compost soil purchased from Semillas Batlle company (Barcelona, Spain) and stored at 4 ℃ prior to use (detailed in Text S2). The obtained DOM stock solution contained 1062.8 ± 40.7 mg C/L, 225.0 ± 50.8 mg total nitrogen (TN)/L, 151.0 ± 18.7 mg NO_3^--N /L, 1.5 ± 0.2 mg NO_2^--N/L and 10.3 ± 3.9 mg NH_4^+-N/L.

2.2. Column setup and operation

The column-scale rapid sand filter module consisted of three quartz columns with 60 cm in length and 10 cm in diameter (Figs. 1 and S2). The columns were filled with a support layer of 8 cm gravel (granule size: 5–7 mm) and covered by a working layer of 32 cm sand (granule size: 0.8–1.25 mm). Above the sand layer, a supernatant water layer with a height of 10 cm was maintained. Column A was the control column, without the spiking of ammonia and DOM; column B was spiked with DOM up to 6 mg C/L and column C was spiked with ammonia up to 2.5 mg NH_4^+-N/L (Fig. 1). Three columns were run in parallel for 178 days, including one inoculation phase (starting up), one selective enrichment phase (Phase 0) and five experimental phases (Fig. S3). The strategies of inoculation, selective enrichment and spiking were described in Text S3. The columns were run in the dark by being fully covered with aluminum foil to avoid algal growth and OMP photodegradation. Each column was operated in an open headspace and connected with a small glass tube as an overflow weir to obtain a stable effluent flow and supernatant height. Backwashing was conducted when clogging occurred in columns, at least weekly, by backwashing program box. Each filter was backwashed by the pressurized tap water for 5 min.

OMPs were spiked into the feeding at the concentration of approximately 1 μg/L during the experimental phases, where different loading rates of DOM, ammonia and OMPs were applied Table 1). Briefly, high loading rates of DOM or ammonia were applied at Phase I, III and V, while lower ones of DOM or ammonia were set at Phase II and IV. At Phase II, the lower loading rates of DOM or ammonia were achieved by decreasing the initial concentration of DOM and ammonia. Differently, the loading rates of DOM, ammonia and OMPs were achieved by decreasing the volumetric flow velocity at Phase IV, so that the EBCTs were consequently longer than other phases. The pumps were recalibrated at the end of each phase to ensure stable flow rates and EBCTs. The theoretical values of operational parameters in Table 1 were calculated by Eqs. ((1) and (2). The loading ratio of DOM/OMP was determined by Eq. (3).

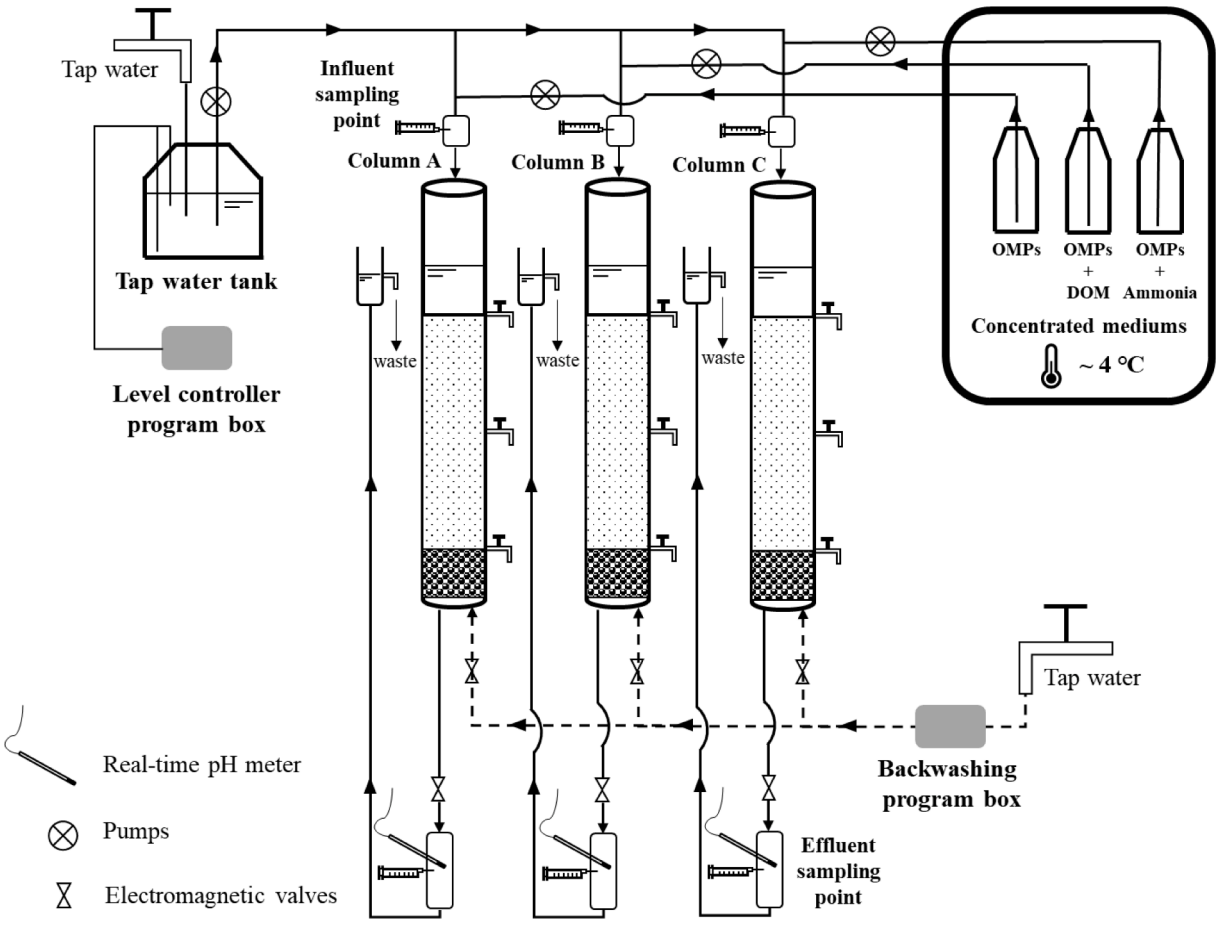

Fig. 1. Schematic of experimental setup.

Table 1
Operational parameters at each experimental phase in three columns.

Substrate loading rates (SLR)															
Phase / Column	Phase I (23 days)			Phase II (22 days)			Phase III (21 days)			Phase IV (22 days)			Phase V (21 days)		
	OMPs (μg/h)	DOM (mg/h)	Ammonia (mg/h)	OMPs (μg/h)	DOM (mg/h)	Ammonia (mg/h)	OMPs (μg/h)	DOM (mg/h)	Ammonia (mg/h)	OMPs (μg/h)	DOM (mg/h)	Ammonia (mg/h)	OMPs (μg/h)	DOM (mg/h)	Ammonia (mg/h)
Control	5.28	–	–	5.28	–	–	5.28	–	–	1.06	–	–	5.28	–	–
DOM	5.28	31.68	–	5.28	10.56	–	5.28	31.68	–	1.76	10.56	–	5.28	31.68	–
Ammonia	5.28	–	13.20	5.28	–	2.64	5.28	–	13.20	1.06	–	2.64	5.28	–	13.20
Substrate concentration in influent															
Phase / Column	Phase I (23 days)			Phase II (22 days)			Phase III (21 days)			Phase IV (22 days)			Phase V (21 days)		
	OMPs (μg/L)	DOM (mg/L)	Ammonia (mg/L)	OMPs (μg/L)	DOM (mg/L)	Ammonia (mg/L)	OMPs (μg/L)	DOM (mg/L)	Ammonia (mg/L)	OMPs (μg/L)	DOM (mg/L)	Ammonia (mg/L)	OMPs (μg/L)	DOM (mg/L)	Ammonia (mg/L)
Control	1	–	–	1	–	–	1	–	–	1	–	–	1	–	–
DOM	1	6	–	1	2	–	1	6	–	1	6	–	1	6	–
Ammonia	1	–	2.5	1	–	0.5	1	–	2.5	1	–	2.5	1	–	2.5
Volumetric flow velocity & EBCTs															
Phase / Column	Phase I (23 days)			Phase II (22 days)			Phase III (21 days)			Phase IV (22 days)			Phase V (21 days)		
	Flow rates (L/h)	EBCTs (h)		Flow rates (L/h)	EBCTs (h)		Flow rates (L/h)	EBCTs (h)		Flow rates (L/h)	EBCTs (h)		Flow rates (L/h)	EBCTs (h)	
Control	5.28	0.48		5.28	0.48		5.28	0.48		1.06	2.38		5.28	0.48	
DOM	5.28	0.48		5.28	0.48		5.28	0.48		1.76	1.43		5.28	0.48	
Ammonia	5.28	0.48		5.28	0.48		5.28	0.48		1.06	2.38		5.28	0.48	

(The loading rates or concentrations of DOM were represented by total organic carbon (mg C/h or mg C/L), the loading rates or concentrations of ammonia were shown by ammonia-nitrogen (mg NH_4^+-N/h or mg NH_4^+-N/L); the experimental loading rates of DOM and ammonia were shown in Figs. S4a and S5a, respectively.).

$$t = \frac{H \times S}{Q \times 10^{-3}} \quad (1)$$

$$SLR = C_{substrate} \times Q \quad (2)$$

$$Y = \frac{SLR_{DOM}}{SLR_{OMP}} \quad (3)$$

where t (h) is empty bed contact time (EBCT); the H (m) is the height of sand layer (without the support layer); S (m^2) represents the cross-sectional area of the column; Q (L/h) is the volumetric flow velocity; SLR (μg/h for OMP, or mg/h for DOM and ammonia) means the substrate loading rate; $C_{substrate}$ (μg/L for OMP, or mg/L for DOM and ammonia) is the substrate concentration in inlet; Y is the loading ratio of DOM/OMP.

To monitor the performance of columns, the multiple chemical parameters (described in Section 2.4) in both influent and effluent were measured every two or three days. During the last week of each experimental phase, the triplicate samples were collected from the top, middle and bottom layers of sand bed to show the vertical removal of contaminants within the columns. At the end of each phase, all columns were drained off, where sand samples (approximately 2 mL) were taken from different layers for further molecular analysis. The removal performance of OMP was represented by the residual OMP in effluent, which was calculated by Eq. (4).

$$R = \left(\frac{C}{C_O}\right) \times 100 \quad (4)$$

where R (%) represents the residual (percentage) of OMPs in effluent; C (ng/L) and C_0 (ng/L) are the concentrations of OMPs in effluent and influent, respectively.

2.3. Chemical analytical methods

The collected samples were filtered through 0.45 μm syringe filters and then stored at 4 ℃ prior to measurement or at −20 ℃ if the storage time was more than one week. Ammonia (NH_4^+-N) and total nitrogen (TN) were measured by Hach TNTplus® Chemistries kits with a spectrophotometer (DR3900, Hach, USA). Nitrate (NO_3^--N) and nitrite (NO_2^--N) were quantified by an ion chromatography (Dionex ICS-2100, Thermo, USA) equipped with an AS17-Column. The DOM concentration was quantified by the total amount of organic carbon (TOC). TOC (non-purgeable organic carbon) concentration was assessed by TOC-L_{CPH} analyzer with an ASI-L autosampler (Shimadzu, Japan). pH values in effluent were recorded by a Datalogger (Consort D230, Belgium) with real-time pH electrodes (ProSense QP108X, the Netherlands). Another set of liquid samples (2 mL) for OMP quantification was mixed with acetonitrile (5% v/v) to avoid OMP sorption onto centrifuge tubes and was centrifuged at 15,000 rpm for 10 min. The supernatants were stored in autosampler vials at −20 ℃ before analysis. OMP quantification was performed on an Ultra High Performance Liquid Chromatography (UHPLC) equipped with a triple quad mass spectrometer (SCIEX Triple Quad™ 5500, USA) (see details in Text S4). The limits of quantification in the sample matrix were 25 ng/L and detection limit was not measured in this experiment.

2.4. Molecular analysis

Genomic DNA was extracted from sand samples (approximately 1000 mg) by DNeasy PowerSoil Kit (QIAGEN, Hilden, Germany). The concentration and quality of extracted DNA were measured by a NanoDrop spectrophotometer (Thermo Fisher Scientific, ND-2000, USA). DNA samples were stored at −80 ℃ prior to further analysis. Quantitative PCR (qPCR) was used to quantify the copy numbers of total bacterial 16S rRNA gene (representing total bacteria), *amo*A gene coding for ammonia monooxygenase (AMO) enzyme (representing nitrifying bacteria) (Fowler et al., 2018) and three functional genes involved in pesticide biodegradation, including *tfdA* gene involving in 2,4-D biodegradation (Bælum et al., 2008) and *rdpA* and *sdpA* genes responsible for mecoprop degradation (Feld et al., 2016). Each sample was assayed in triplicates by using a C1000 Thermal Cycler (CFX384 Real-Time system, Bio-Rad Laboratories, USA) with iQTM SYBR Green Supermix (Bio-Rad Laboratories, USA). Standard calibration curves were obtained by using gradient concentrations of plasmid DNA containing the target genes. Further information of primers and cycling sequences applied for qPCR were listed in Table S5.

2.5. Kinetic analysis

Kinetic analysis was used to compare OMP biodegradation rates in different phases. Previous studies demonstrated the microbial transformation of pollutants in biofilms followed pseudo-first-order kinetic model (Smook et al., 2008; Zearley and Summers, 2012). In addition, the biodegradation pattern of trace organic pollutants that are not supporting bacterial growth is best fit by pseudo-first-order kinetic model (Schmidt et al., 1985). Therefore, the pseudo-first-order kinetic models (Eq. (5)) was applied to analyze the biodegradation processes of OMPs under different conditions in this study.

$$\ln(C/C_0) = -k \cdot t \quad (5)$$

where C (ng/L) and C_0 (ng/L) were the concentrations of OMPs in effluent and influent; t (h) was EBCT; and k (h^{-1}) was the first-order rate constant.

2.6. Statistical analysis

The student's test (t-test) was carried out to identify the significance of differences for OMP removal among three columns and OMP biodegradation kinetic constants in different operational phases. All the statistical analyses were performed by using R (version 4.1.0).

3. Results and discussion

3.1. The activities of heterotrophic and nitrifying bacteria affect OMP removal

The adsorption batch assay (see details in Text S5) showed that adsorption to sand did not significantly contribute to the removal of selected OMPs (Fig. S6), as was also confirmed by other studies (Zearley and Summers, 2012). Biodegradation was therefore proposed as the main removal process of OMPs in columns. Ten compounds were negligibly removed throughout the experiments, and were thus regarded as recalcitrant compounds in this study (Fig. S7).

The addition of DOM or ammonia dictated the activity of heterotrophic or nitrifying bacteria with varied biodegradation capacities for paracetamol, benzotriazole, 2,4-D and mecoprop. The biodegradation of paracetamol, 2,4-D and mecoprop was stimulated by the addition of DOM, as their median removal increased from 20.6% (Fig. 2a), 32.5% (Fig. 2c) and 26.4% (Fig. 2d) in the control column to 62.4% (Fig. 2a), 52.6% (Fig. 2c) and 54.4% (Fig. 2d) in the DOM column, respectively. In contrast, their biodegradation was suppressed in the ammonia column, where the median removal decreased to 0.8% for paracetamol (Fig. 2a), 2.9% for 2,4-D (Fig. 2c) and −1.8% for mecoprop (Fig. 2d). The addition of ammonia combined with a limited DOM feeding in the ammonia column might allow nitrifying bacteria to outcompete the heterotrophic degraders. Therefore, the biodegradation of paracetamol, 2,4-D and mecoprop was most likely attributed to the activity of the heterotrophic community rather than that of nitrifying community.

In contrast to the aforementioned three OMPs, benzotriazole showed an opposite removal behavior with the addition of DOM or ammonia (Fig. 2b). Benzotriazole biodegradation was inhibited by the addition of

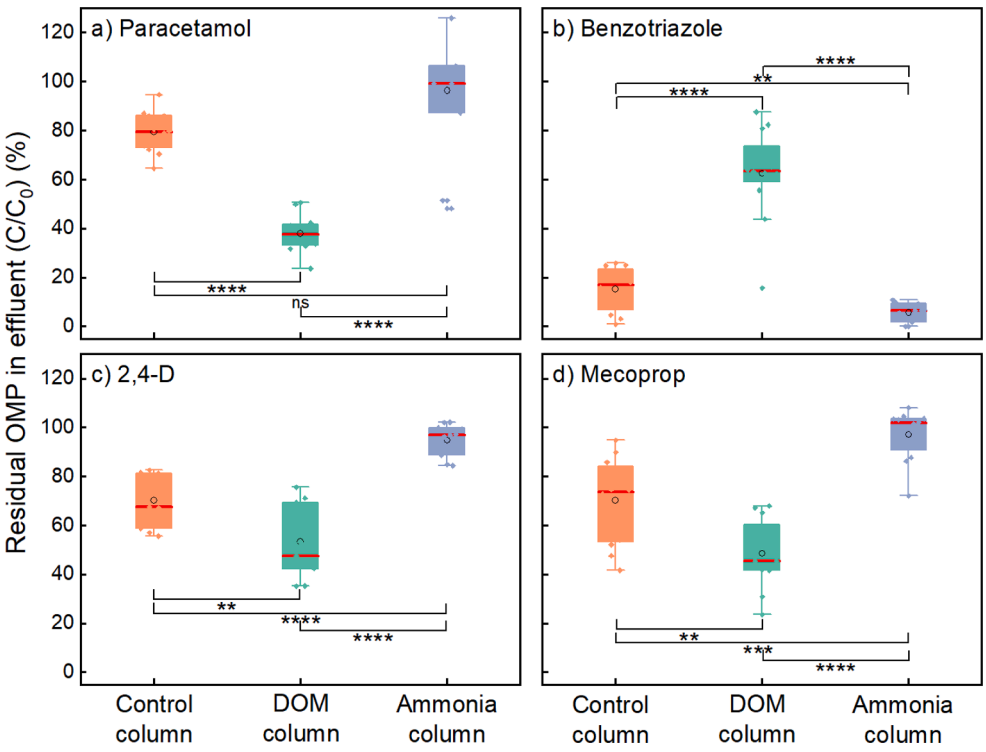

Fig. 2. OMP removal in different columns in the first experimental phase (red lines indicate median; boxes show interquartile range; whiskers represent minimum and maximum non-outlying values; solid diamond points show the data points individually, $n = 12$). Student's test (*t*-test) was used to analyze the significance of each paired group for OMP removal, "ns" indicates no significant difference with *p*-value > 0.05; "*" means *p*-value is 0.01–0.05; "**" means *p*-value is 0.001–0.01; "***" means *p*-value is 0.0001–0.001; "****" means *p*-value is < 0.0001.

DOM, with a median removal of 36.5% in the DOM column as compared to the control column with 83.0% (Fig. 2b). The inhibited biodegradation of benzotriazole in the DOM column could be due to substrate competition between DOM and benzotriazole. Previous studies indicated that the presence of biodegradable DOM could reduce microbial biodegradation preference for certain OMPs (e.g., caffeine) due to the substrate competition (He et al., 2018). Therefore, microorganisms able to degrade benzotriazole may prefer to metabolize biodegradable DOM instead of benzotriazole if excess DOM is available. In addition, benzotriazole biodegradation was enhanced by the addition of ammonia, with a median removal of 93.5% (Fig. 2b). The improved removal of benzotriazole under nitrification conditions was most likely due to the autotrophic co-metabolisms. Trejo-Castillo et al. (2021) reported that benzotriazole could be co-metabolically biodegraded in nitrifying cultures, and increasing the initial ammonia concentration resulted in an increase in benzothiazole co-metabolism. It was also observed that the ammonium monooxygenase (AMO) enzyme can oxidize a broad range of organic compounds by hydroxylating alkyl groups or aromatic ring (Fernandez-Fontaina et al., 2016). We therefore conclude that nitrifying bacteria may contribute to benzotriazole biodegradation.

3.2. DOM loading patterns dictate OMP biodegradation rates

3.2.1. The loading ratio of DOM/benzotriazole determines benzotriazole biodegradation rates

Lower DOM loading rates benefited benzotriazole biodegradation. The average removal of benzotriazole was 20.1 ± 14.2% in the phases with high DOM loading rates (31.4 ± 4.4 mg C·h^{-1}), whereas was 48.1 ± 9.2% in the phases with low DOM loading rates (11.8 ± 2.6 mg C·h^{-1}) (Fig. S8a). There was a significant difference (*p*-value = 6.99 × 10^{-6}, *t*-test) in benzotriazole removal between the high DOM loading phases and the low DOM loading phases. The negative effects of DOM loading rates on benzotriazole biodegradation were consistent with the finding in Section 3.1, where the presence of DOM negatively affect benzotriazole removal. We subsequently examined the effects of substrate competition on the biodegradation rate of benzotriazole. The loading ratio of DOM/benzotriazole represents the level of substrate competition, while biodegradation kinetic constants show the biodegradation rate. The results revealed that biodegradation kinetic constant of benzotriazole was highest in Phase II, where the loading ratio of DOM/benzotriazole is lowest (Fig. 3). In addition, vertical removal data showed that more benzotriazole was removed in the bottom-half of DOM column (Fig. S8b). This could be the result of a lower loading ratio of DOM/benzotriazole due to partial DOM consumption in the top-half of the column. Thus, the lower loading ratio of DOM/Benzotriazole established a condition with less substrate competition, which was beneficial for benzotriazole biodegradation.

An improved removal of benzotriazole under carbon-limited conditions was also observed in sequential managed aquifer recharge systems (Müller et al., 2017; Hellauer et al., 2018a, 2018b). In these systems, benzotriazole was recalcitrant in the first aquifer passage (Hellauer et al., 2018a, 2018b), where higher concentrations of degradable DOM were present (Regnery et al., 2016). Benzotriazole was efficiently biodegraded in the second aquifer passage (Hellauer et al., 2018a, 2018b), where water was carbon-depleted as the easily biodegradable DOM was consumed in the first passage. These findings combined with our results could verify the fact that DOM overloading is disadvantageous for benzotriazole biodegradation due to the stronger substrate competition. The surplus biodegradable DOM increased microbial preferences for utilizing DOM instead of benzotriazole. In addition, DOM consists of a range of organic molecules with different biodegradation rates, thus DOM containing different biodegradable fractions may show variable biodegradability and hence affect the substrate competition.

3.2.2. DOM loading enhances heterotrophic bacteria growth for paracetamol biodegradation

Long-term operation resulted in the growth of heterotrophic communities to degrade paracetamol in both the control and the DOM column. Biodegradation kinetic constants of paracetamol gradually increased over the course of the 109 days of OMP exposure (Fig. 4a). The temporary decrease in Phase IV was most likely due to the longer EBCTs, which will be discussed in Section 3.4. It has been widely reported that OMP biodegradation was increased after exposure to OMPs for an adaption period in filtration system (Hedegaard et al., 2014; Bertelkamp

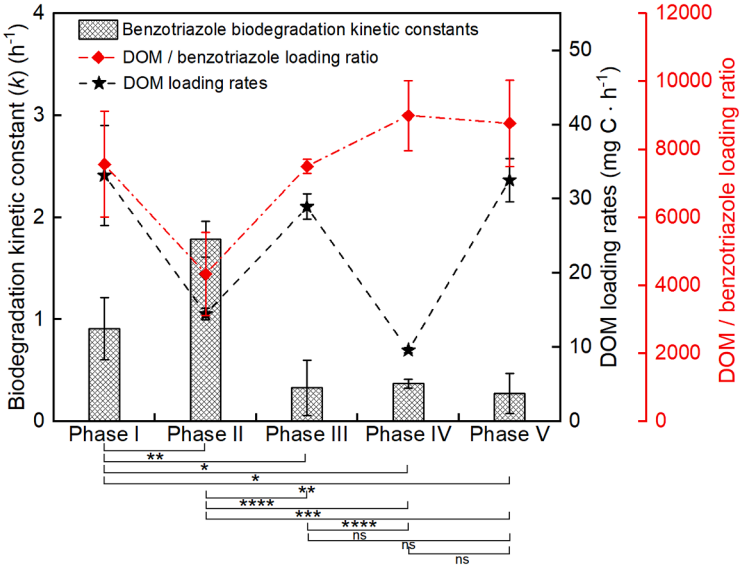

Fig. 3. Benzotriazole biodegradation rates under different loading rates of DOM and different loading ratios of DOM and benzotriazole. The average values of the last-week data points are used as the steady value of each phase; whiskers show the standard deviations of average values, $4 \leq n \leq 5$. Student's test (*t*-test) was used to check the significance of each paired phase for benzotriazole biodegradation kinetic constant (k), "ns" indicates no significant difference with *p*-value > 0.05; "*" means *p*-value is 0.01–0.05; "**" means *p*-value is 0.001–0.01; "***" means *p*-value is 0.0001–0.001; "****" means *p*-value is < 0.0001.

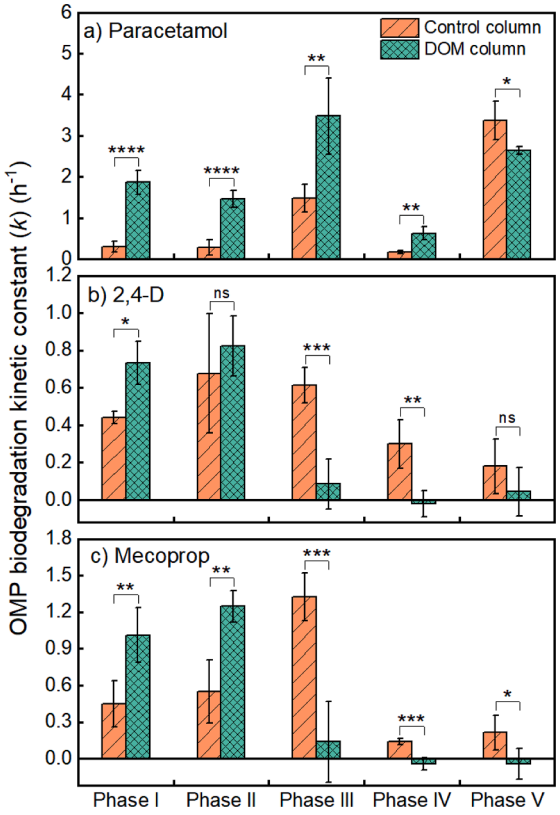

Fig. 4. The biodegradation rates of (a) paracetamol, (b) 2,4-D and (c) mecoprop in the control and the DOM column. The average values of the last-week data points represent the steady value of each phase; whiskers show the standard deviations of average values, $4 \leq n \leq 5$. Student's test (*t*-test) was used to check the significance of each paired group for OMP biodegradation kinetic constant (k), "ns" indicates no significant difference with *p*-value > 0.05; "*" means *p*-value is 0.01–0.05; "**" means *p*-value is 0.001–0.01; "***" means *p*-value is 0.0001–0.001; "****" means *p*-value is < 0.0001.

et al., 2016). Modrzyński et al. (2021) found that the biodegradation of paracetamol was completed after 15 weeks microbial adaption in a column-scale aquifer. The discussion in Section 3.1 suggested that paracetamol biodegradation was contingent on the activity of heterotrophic community. Thus, the microbial adaption for paracetamol biodegradation could be the proliferation of heterotrophic degraders.

The feeding with DOM promoted the growth of heterotrophic degrader and hence shortened the adaption time. During the first three phases, the biodegradation kinetic constants of paracetamol in DOM column were 6.2-fold, 5.2-fold and 2.3-fold compared to the ones in the control column (Fig. 4a). In addition, the kinetic constants reached to above 3.0 h^{-1} within three phases (66 days) in the DOM column, while it needed five phases (109 days) in the control column to reach the same extent (Fig. 4a). The longer adaption time in control column might be due to the slower growth of heterotrophs with limited biodegradable DOM. The copy numbers of total bacterial 16S rRNA gene in the control column were less than in the DOM column at the end of Phase 0 and Phase I (Fig. S9b), suggesting the bacterial community grew up more slowly in the control column. Additionally, most of paracetamol was removed at the top-half of the DOM column (Fig. S9a) with more available DOM and higher bacterial abundance (Fig. S9b), confirming the biodegradation of paracetamol required a sufficient activity of the heterotrophic community. Therefore, feeding with DOM can contribute to the establishment of enough heterotrophic degraders, and hence, shorten the microbial adaption time for paracetamol biodegradation.

3.2.3. 2,4-D and mecoprop biodegradation decreased due to substrate competition

The feeding with DOM temporarily supported 2,4-D and mecoprop biodegradation in Phase I and II, while the biodegradation rates of both herbicides decreased after Phase II in the DOM column and after Phase III in the control column (Fig. 4b and c). In our experiment, biodegradation of 2,4-D and mecoprop at concentrations of 1 μg/L was most likely under nongrowth kinetics (Torang et al., 2003). Thus, feeding with DOM could improve herbicide biodegradation rates by supporting the growth of the herbicide degrader. Previous studies suggested that the reduced OMP biodegradation activity was associated with the loss of degrader cells (Albers et al., 2015; Horemans et al., 2017). The bacterial loss mechanisms include loss from backwashing, from protozoan predation and from starvation (Albers et al., 2015). However, the reduction in biodegradation activity in our reactors could not be explained by the loss of degraders, since the abundances of the *tfdA* gene (involving in 2, 4-D biodegradation) (Fig. S10a) and the *sdpA* gene (required for mecoprop biodegradation) (Fig. S10b) were at a stable level or even increased in the last three phases. The *rdpA* gene was not detectable in our study, which agrees with other reports (Paulin et al., 2011; Feld et al., 2016). A potential mechanism for diminished biodegradation of 2,4-D and

mecoprop during long term column operation is substrate competition. In the adaptive phase without OMP spiking (Phase 0), the abundance of *tfdA* and *sdpA* genes was higher in the DOM column than in the control column (Fig. S10), implying that the 2,4-D and mecoprop degraders can grow on DOM. As a result, the specific degrading microorganisms might adapt to DOM-dependent growth instead of utilizing 2,4-D and mecoprop as carbon sources. This microbial adaption was delayed in the control column (Fig. 4b and c) and might be the result of the lower degradability of tap water DOM compared with compost DOM. Therefore, the feeding of DOM temporarily benefits 2,4-D and mecoprop biodegradation by providing an extra carbon source for degrader growth, but the biodegradation activity diminished with time due to substrate competition after a long-term operation.

3.3. Nitrification rates dictate benzotriazole biodegradation rates

The removal behavior of benzotriazole in ammonia column revealed the effect of ammonia loading rates on benzotriazole biodegradation. The removal efficiency was improved with the increase in ammonia loading rates. The high ammonia loading rates (13.4 ± 1.0 mg NH_4^+-N·h^{-1}) resulted in an average removal of 72.4 ± 16.2%, while the removal for the low loading rates (2.7 ± 0.3 mg NH_4^+-N·h^{-1}) was 32.2 ± 9.0% (Fig. S11a). The benzotriazole removal was significantly different (p-value = 4.47 × 10^{-7}, t-test) between the high ammonia loading phases and the low ammonia loading phases. Furthermore, ammonia loading rates positively affect benzotriazole biodegradation rates, with an average kinetic constant of 3.2 ± 1.6 h^{-1} in Phase I, III and V compared with 0.4 ± 0.4 h^{-1} in Phase II and IV (Fig. 5a). The nitrification rates appear strongly correlated with ammonia loading rates (Fig. 5a), as previously suggested by Lee et al. (2014). Hence, the activity of nitrifying bacteria dictates benzotriazole biodegradation rates, which is verified by the vertical removal pattern of benzotriazole and the abundance of *amoA* gene with depth. Fig. 5b represents how the majority of benzotriazole was removed in the top-half of column, where the nitrification process mainly took place (Fig. 5c). Moreover, the copy numbers of *amoA* genes, representing the abundance of nitrifying bacteria (Fowler et al., 2018), was higher in the top layer than in the bottom layer (Fig. 5d). The negligible nitrite formation indicates the presence of complete ammonia-oxidizing (comammox) nitrifier in the column (Figs. 5c and S12). It has been reported that comammox nitrifier, like *Nitrospira*, dominated the nitrifying community in field RSFs (Fowler et al., 2018; Poghosyan et al., 2020; Hu et al., 2020; Wang et al., 2022). These outcomes show that the high loading rates of ammonia can promote benzotriazole biodegradation rates by stimulating the activity of nitrifying bacteria.

3.4. Effects of EBCT on OMP biodegradation rates

In this study, control column was fed with neither additional ammonia nor biodegradable DOM, where EBCT was therefore the sole

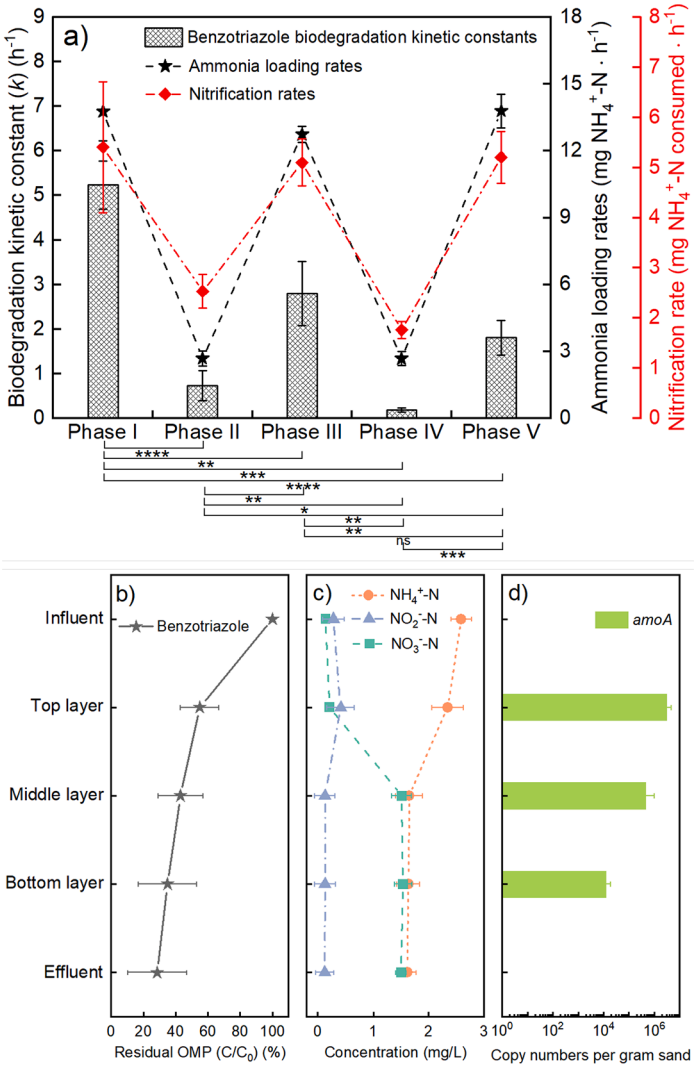

Fig. 5. Benzotriazole biodegradation in the ammonia column. (a) Benzotriazole biodegradation rates under different nitrification activities. The average values of the last-week data points are used as the steady value of each phase; whiskers show the standard deviations of average values, $4 \leq n \leq 5$. Student's test (t-test) was used to check the significance of each paired phase for benzotriazole biodegradation kinetic constant (k), "ns" indicates no significant difference with p-value > 0.05; "*" means p-value is 0.01–0.05; "**" means p-value is 0.001–0.01; "***" means p-value is 0.0001–0.001; "****" means p-value is < 0.0001. (b) the vertical residual concentration of benzotriazole through sand bed in Phases I, III and V with high ammonia loading rates, $n = 8$; (c) the vertical consumption of ammonia (NH_4^+-N) and production of nitrite (NO_2^--N) and nitrate (NO_3^--N) in Phases I, III and V with high ammonia loading rates, $n = 9$; d) the average abundance of amoA genes in different layers of sand bed at the end of Phases I, III and V, $n = 9$.

controlled changing factor during all the phases of the experiment (Table 1). Therefore, the biodegradation performances in control column were used for understanding the impacts of EBCT on OMP biodegradation rates. A prolonged EBCT limits the biodegradation activities of paracetamol and benzotriazole, as a 5× longer EBCT in phase IV resulted in lower biodegradation kinetic constants for paracetamol and benzotriazole (Fig. 6a and b). The prolonged EBCTs can reduce the microbial activity by limiting substrate loading rates and hence result in inhibitory effects on OMP biodegradation (Paredes et al., 2016; Wang et al., 2021). Our results showed that paracetamol biodegradation was contingent on the activity of the heterotrophic community (Figs. 2a and 4a). Therefore, the longer EBCT may limit the activity of heterotrophic degraders by decreasing DOM loading rates, and thus reduce the biodegradation rates of paracetamol. The prolonged EBCT reduced the loading rates of both DOM and benzotriazole, and hence, resulted in a similar competitive condition for benzotriazole biodegradation. This demonstrates that the reduced activity for benzotriazole biodegradation with prolonged EBCT may result from the deceased substrate loading rates rather than the substrate competition.

In contrast, a longer EBCT improved metformin biodegradation efficiency in all the columns (Fig. S13). Especially in the control column, the removal efficiency of metformin during Phase IV was 46.4 ± 12.8%, while the average removal during other phases were 2.5 ± 7.4% (Fig. S13a). Moreover, the biodegradation rate of metformin at Phase IV was the highest, with a kinetic constant of 0.3 ± 0.1 h^{-1}, versus an average constant of 0.06 ± 0.2 h^{-1} for other phases (Fig. 6c). The biodegradation kinetic constant of metformin was lower than paracetamol and benzotriazole, indicating a lower biodegradation rate for metformin (Fig. 6). In addition, metformin was previously categorized as not a readily biodegradable compound (Trautwein and Kümmerer, 2011) and its biodegradation thus required long residence times (Scheurer et al., 2012). A microbial degradation of metformin occurred in a drinking water aquifer with a residence time of about one year (Scheurer et al., 2012), while another considerable biodegradation of metformin (more than 85%) was achieved in a managed aquifer recharge with a travel time of 4.08 and 11.76 h (Hellauer et al., 2018a). Therefore, a longer EBCT may benefit metformin biodegradation in RSFs, as the degraders need sufficient time to induce biotransformation.

4. Conclusion and field implications

The use of RSFs to biodegrade OMPs is receiving increasing interest but is challenging, as biodegradation patterns of OMPs under multiple operational conditions are not yet sufficiently understood. To the best of our knowledge, this is the first paper examining OMP biodegradation behaviors vis-à-vis substrate and contaminant loading patterns in a continuous filter system with multiple OMPs at trace concentrations. The feed of DOM promotes paracetamol biodegradation by supporting the growth of heterotrophic degraders, while inhibiting benzotriazole biodegradation due to substrate competition. The substrate competition also reduces the biodegradation of 2,4-D and mecoprop with time. We therefore propose two mechanisms for OMP biodegradation by heterotrophic populations: (i) paracetamol is degraded by general heterotrophic communities, where the generated enzymes for DOM utilization are also capable of degrading paracetamol; (ii) benzotriazole, 2,4-D and mecoprop are degraded by specific degraders that can utilize both DOM and OMPs. High DOM loading rates can therefore reduce the microbial preference for OMPs via substrate competition. Two field strategies can hereby be envisioned to improve the biodegradation of benzotriazole, 2,4-D and mecoprop. First, two filter units can be designed in series, where a majority of biodegradable DOM can be consumed in the primary unit, while the secondary filter can provide favorable, low DOM conditions for OMP biodegradation. Instead of building a secondary filter unit, extending the sand bed can be another option to create a low

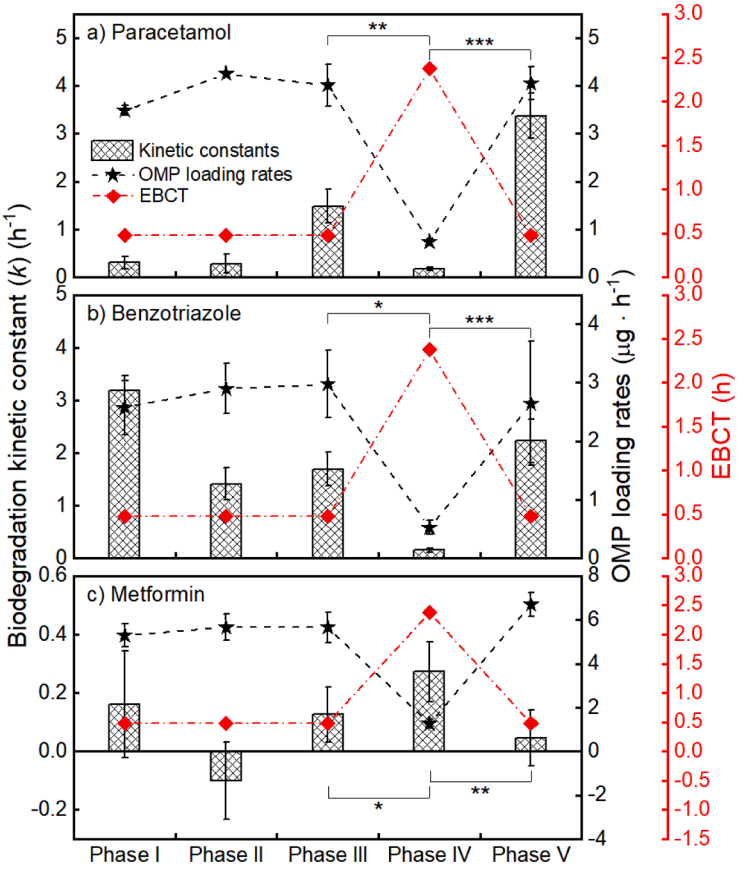

Fig. 6. The biodegradation rates of (a) paracetamol, (b) benzotriazole and (c) metformin at different EBCTs in the control column. The average values of the last-week data points represent the steady value of each phase; whiskers show the standard deviations of average values, $4 \leq n \leq 5$. The negative values were likely due to the instrument accuracy and measurement errors when OMP removal was negligible. Student's test (*t*-test) was used to check the significance of each paired phase for OMP biodegradation kinetic constant (k), "ns" indicates no significant difference with *p*-value > 0.05; "*" means *p*-value is 0.01–0.05; "**" means *p*-value is 0.001–0.01; "***" means *p*-value is 0.0001–0.001; "****" means *p*-value is < 0.0001.

DOM condition. It is assumed that assimilable DOM is utilized by communities in the upper part of the filter, making the lower part of the filter suitable for benzotriazole, 2,4-D, and mecoprop biodegradation. Additionally, we need to consider the effects of DOM biodegradability on OMP biodegradation in practice. The DOM in the field inlet can be more recalcitrant than the compost DOM used in this study. Thus, the substrate competition may be less pronounced in field RSF. In contrast, adding biodegradable DOM in influent is a possible solution to enhance microbial elimination of paracetamol. In this case, the residual DOM in effluent (if any) needs to be strictly monitored and removed to ensure proper drinking water quality.

Stimulating nitrification enhances the co-metabolism of benzotriazole, but inhibits biodegradation of paracetamol, 2,4-D and mecoprop. Therefore, a promising alternative for improving benzotriazole biodegradation is to boost nitrifying bacteria growth by adding additional ammonia in RSFs. To avoid the excess nitrate production or increased oxygen consumption in daily operation, periodically backwashing the sand bed with ammonia could be an attractive strategy. Similarly, as aeration is an upstream facility for RSFs in DWPPs, limiting nitrification there can improve ammonia loading amounts, thereby supporting nitrification activity in RSFs. However, it should be noted that certain OMPs, like paracetamol, 2,4-D and mecoprop, are mainly degraded by heterotrophic bacteria. Therefore, an improving nitrification activity may be detrimental for their removal, as autotrophs will dominate over heterotrophic communities.

Prolonging EBCT improves metformin removal by providing sufficient contact time, but reduces biodegradation rates of paracetamol and benzotriazole due to the substrate supply limitation. It seems unrealistic to guarantee a satisfactory removal of multiple compounds with one EBCT, however, EBCTs need to be prolonged when slow biodegrading compounds are present in the inlet water. To prevent the reduced biodegradation rate of other compounds from decreasing substrate loading rates, a thicker sand bed could be an option to offer a longer EBCT without reducing flow velocity. Overall, this research contributes to an improved understanding of how substrate loading patterns determine OMP biodegradation activity in RSFs, providing a key foundation for optimizing RSFs for the removal of OMPs from drinking water.

CRediT authorship contribution statement

Jinsong Wang: Conceptualization, Methodology, Investigation, Formal analysis, Data curation, Software, Writing – original draft, Visualization, Project administration. **Baptiste A.J. Poursat:** Formal analysis, Writing – review & editing, Supervision. **Jiahao Feng:** Methodology, Investigation, Writing – review & editing. **David de Ridder:** Resources, Writing – review & editing, Supervision. **Chen Zhang:** Formal analysis, Writing – review & editing. **Albert van der Wal:** Writing – review & editing, Supervision, Funding acquisition. **Nora B. Sutton:** Conceptualization, Methodology, Formal analysis, Writing – review & editing, Supervision, Funding acquisition, Project administration.

Declaration of Competing Interest

The authors declare that they have no known competing financial interests or personal relationships that could have appeared to influence the work reported in this paper.

Data availability

Data will be made available on request.

Acknowledgments

The authors are sincerely thankful to Evides Water Company N.V. and China Scholarship Council (CSC, File No. 201804910659) for financial support. The authors acknowledge Livio Carlucci for offering analytical support, and Vinnie de Wilde for his help with the column operation. We are also thankful to Hauke Smidt (Lab of Microbiology, Wageningen University & Research) for his help with molecular experiments and Dandan Liu for her suggestions for this work. Finally, we thank Anran Li, Laura Piai and Zhaolu Feng for proofreading the manuscript.

Supplementary materials

Supplementary material associated with this article can be found, in the online version, at doi:10.1016/j.watres.2022.118832.

References

Albers, C.N., Ellegaard-Jensen, L., Hansen, L.H., Sørensen, S.R., 2018. Bioaugmentation of rapid sand filters by microbiome priming with a nitrifying consortium will optimize production of drinking water from groundwater. Water Res. 129, 1–10.
Albers, C.N., Feld, L., Ellegaard-Jensen, L., Aamand, J., 2015. Degradation of trace concentrations of the persistent groundwater pollutant 2,6-dichlorobenzamide (BAM) in bioaugmented rapid sand filters. Water Res. 83, 61–70.
Bar-Zeev, E., Belkin, N., Liberman, B., Berman, T., Berman-Frank, I., 2012. Rapid sand filtration pretreatment for SWRO: microbial maturation dynamics and filtration efficiency of organic matter. Desalination 286, 120–130.
Bælum, J., Nicolaisen, M.H., Holben, W.E., Strobel, B.W., Sørensen, J., Jacobsen, C.S., 2008. Direct analysis of tfdA gene expression by indigenous bacteria in phenoxy acid amended agricultural soil. ISME J. 2 (6), 677–687.
Ben, W., Zhu, B., Yuan, X., Zhang, Y., Yang, M., Qiang, Z., 2018. Occurrence, removal and risk of organic micropollutants in wastewater treatment plants across China: comparison of wastewater treatment processes. Water Res. 130, 38–46.
Benner, J., Helbling, D.E., Kohler, H.P.E., Wittebol, J., Kaiser, E., Prasse, C., Ternes, T.A., Albers, C.N., Aamand, J., Horemans, B., et al., 2013. Is biological treatment a viable alternative for micropollutant removal in drinking water treatment processes? Water Res. 47 (16), 5955–5976.
Bertelkamp, C., Verliefde, A.R.D., Schoutteten, K., Vanhaecke, L., Vanden Bussche, J., Singhal, N., van der Hoek, J.P., 2016. The effect of redox conditions and adaptation time on organic micropollutant removal during river bank filtration: a laboratory-scale column study. Sci. Total Environ. 544, 309–318.
Björklund, E., Anskjær, G.G., Hansen, M., Styrishave, B., Halling-Sørensen, B., 2011. Analysis and environmental concentrations of the herbicide dichlobenil and its main metabolite 2,6-dichlorobenzamide (BAM): a review. Sci. Total Environ. 409 (12), 2343–2356.
Combarros, R.G., Rosas, I., Lavín, A.G., Rendueles, M., Díaz, M., 2014. Influence of biofilm on activated carbon on the adsorption and biodegradation of salicylic acid in wastewater. Water Air Soil Pollut. 225 (2), 1–12.
Elhadi, S.L.N., Huck, P.M., Slawson, R.M., 2006. Factors affecting the removal of geosmin and MIB in drinking water biofilters. J. Am. Water Works Assoc. 98 (8), 108–119.
Feld, L., Nielsen, T.K., Hansen, L.H., Aamand, J., Albers, C.N., 2016. Establishment of bacterial herbicide Degraders in a rapid sand filter for bioremediation of phenoxypropionate-polluted groundwater. Appl. Environ. Microbiol. 82 (3), 878–887.
Fernandez-Fontaina, E., Gomes, I.B., Aga, D.S., Omil, F., Lema, J.M., Carballa, M., 2016. Biotransformation of pharmaceuticals under nitrification, nitratation and heterotrophic conditions. Sci. Total Environ. 541, 1439–1447.
Fowler, S.J., Palomo, A., Dechesne, A., Mines, P.D., Smets, B.F., 2018. Comammox nitrospira are abundant ammonia oxidizers in diverse groundwater-fed rapid sand filter communities. Environ. Microbiol. 20 (3), 1002–1015.
Hack, N., Reinwand, C., Abbt-Braun, G., Horn, H., Frimmel, F.H., 2015. Biodegradation of phenol, salicylic acid, benzenesulfonic acid, and iomeprol by Pseudomonas fluorescens in the capillary fringe. J. Contam. Hydrol. 183, 40–54.
He, Y., Langenhoff, A.A.M., Comans, R.N.J., Sutton, N.B., Rijnaarts, H.H.M., 2018. Effects of dissolved organic matter and nitrification on biodegradation of pharmaceuticals in aerobic enrichment cultures. Sci. Total Environ. 630, 1335–1342.
Hedegaard, M.J., Arvin, E., Corfitzen, C.B., Albrechtsen, H.J., 2014. Mecoprop (MCPP) removal in full-scale rapid sand filters at a groundwater-based waterworks. Sci. Total Environ. 499, 257–264.
Hedegaard, M.J., Deliniere, H., Prasse, C., Dechesne, A., Smets, B.F., Albrechtsen, H.J., 2018. Evidence of co-metabolic bentazone transformation by methanotrophic enrichment from a groundwater-fed rapid sand filter. Water Res. 129, 105–114.
Hellauer, K., Karakurt, S., Sperlich, A., Burke, V., Massmann, G., Hübner, U., Drewes, J. E., 2018a. Establishing sequential managed aquifer recharge technology (SMART) for enhanced removal of trace organic chemicals: experiences from field studies in Berlin, Germany. J. Hydrol. (Amst) 563, 1161–1168.
Hellauer, K., Uhl, J., Lucio, M., Schmitt-Kopplin, P., Wibberg, D., Hübner, U., Drewes, J. E., 2018b. Microbiome-triggered transformations of trace organic chemicals in the

presence of effluent organic matter in managed aquifer recharge (MAR) systems. Environ. Sci. Technol. 52 (24), 14342–14351.
Horemans, B., Raes, B., Vandermaesen, J., Simanjuntak, Y., Brocatus, H., T'Syen, J., Degryse, J., Boonen, J., Wittebol, J., Lapanje, A., Sørensen, S.R., Springael, D., 2017. Biocarriers improve bioaugmentation efficiency of a rapid sand filter for the treatment of 2,6-dichlorobenzamide-contaminated drinking water. Environ. Sci. Technol. 51 (3), 1616–1625.
Hu, W., Liang, J., Ju, F., Wang, Q., Liu, R., Bai, Y., Liu, H., Qu, J., 2020. Metagenomics unravels differential microbiome composition and metabolic potential in rapid sand filters purifying surface water versus groundwater. Environ. Sci. Technol. 54 (8), 5197–5206.
Kim, J., Kang, B., 2008. DBPs removal in GAC filter-adsorber. Water Res. 42 (1–2), 145–152.
Košutić, K., Furač, L., Sipos, L., Kunst, B., 2005. Removal of arsenic and pesticides from drinking water by nanofiltration membranes. Sep. Purif. Technol. 42 (2), 137–144.
Lee, C.O., Boe-Hansen, R., Musovic, S., Smets, B., Albrechtsen, H.J., Binning, P., 2014. Effects of dynamic operating conditions on nitrification in biological rapid sand filters for drinking water treatment. Water Res. 64, 226–236.
Liu, L., Helbling, D.E., Kohler, H.P.E., Smets, B.F., 2014. A model framework to describe growth-linked biodegradation of trace-level pollutants in the presence of coincidental carbon substrates and microbes. Environ. Sci. Technol. 48 (22), 13358–13366.
Maeng, S.K., Sharma, S.K., Abel, C.D.T., Magic-Knezev, A., Amy, G.L., 2011. Role of biodegradation in the removal of pharmaceutically active compounds with different bulk organic matter characteristics through managed aquifer recharge: batch and column studies. Water Res. 45 (16), 4722–4736.
Modrzyński, J.J., Aamand, J., Wittorf, L., Badawi, N., Hubalek, V., Canelles, A., Hallin, S., Albers, C.N., 2021. Combined removal of organic micropollutants and ammonium in reactive barriers developed for managed aquifer recharge. Water Res. 190, 116669.
Müller, J., Drewes, J.E., Hübner, U., 2017. Sequential biofiltration – a novel approach for enhanced biological removal of trace organic chemicals from wastewater treatment plant effluent. Water Res. 127, 127–138.
Ormad, M.P., Miguel, N., Claver, A., Matesanz, J.M., Ovelleiro, J.L., 2008. Pesticides removal in the process of drinking water production. Chemosphere 71 (1), 97–106.
Paredes, L., Fernandez-Fontaina, E., Lema, J.M., Omil, F., Carballa, M., 2016. Understanding the fate of organic micropollutants in sand and granular activated carbon biofiltration systems. Sci. Total Environ. 551-552, 640–648.
Paulin, M.M., Nicolaisen, M.H., Sørensen, J., 2011. (R,S)-dichlorprop herbicide in agricultural soil induces proliferation and expression of multiple dioxygenase-encoding genes in the indigenous microbial community. Environ. Microbiol. 13 (6), 1513–1523.
Phillips, P.J., Schubert, C., Argue, D., Fisher, I., Furlong, E.T., Foreman, W., Gray, J., Chalmers, A., 2015. Concentrations of hormones, pharmaceuticals and other micropollutants in groundwater affected by septic systems in New England and New York. Sci. Total Environ. 512-513, 43–54.
Piai, L., Dykstra, J.E., Adishakti, M.G., Blokland, M., Langenhoff, A.A.M., van der Wal, A., 2019. Diffusion of hydrophilic organic micropollutants in granular activated carbon with different pore sizes. Water Res. 162, 518–527.
Poghosyan, L., Koch, H., Frank, J., van Kessel, M.A.H.J., Cremers, G., van Alen, T., Jetten, M.S.M., Op den Camp, H.J.M., Lücker, S., 2020. Metagenomic profiling of ammonia- and methane-oxidizing microorganisms in two sequential rapid sand filters. Water Res. 185, 116288.
Rattier, M., Reungoat, J., Keller, J., Gernjak, W., 2014. Removal of micropollutants during tertiary wastewater treatment by biofiltration: role of nitrifiers and removal mechanisms. Water Res. 54, 89–99.
Regnery, J., Wing, A.D., Kautz, J., Drewes, J.E., 2016. Introducing sequential managed aquifer recharge technology (SMART) – from laboratory to full-scale application. Chemosphere 154, 8–16.
Sarkar, B., Venkateswralu, N., Rao, R.N., Bhattacharjee, C., Kale, V., 2007. Treatment of pesticide contaminated surface water for production of potable water by a coagulation-adsorption-nanofiltration approach. Desalination 212 (1–3), 129–140.
Scheurer, M., Michel, A., Brauch, H.J., Ruck, W., Sacher, F., 2012. Occurrence and fate of the antidiabetic drug metformin and its metabolite guanylurea in the environment and during drinking water treatment. Water Res. 46 (15), 4790–4802.
Schmidt, S.K., Simkins, S., Alexander, M., 1985. Models for the kinetics of biodegradation of organic compounds not supporting growth. Appl. Environ. Microbiol. 50 (2), 323–331.
Schwarzenbach, R.P., Escher, B.I., Fenner, K., Hofstetter, T.B., Johnson, C.A., von Gunten, U., Wehrli, B., 2006. The challenge of micropollutants in aquatic systems. Science 313 (5790), 1072–1077.
Smook, T.M., Zho, H., Zytner, R.G., 2008. Removal of ibuprofen from wastewater: comparing biodegradation in conventional, membrane bioreactor, and biological nutrient removal treatment systems. Water Sci. Technol. 57 (1), 1–8.
Stratton, R.G., Namkung, E., Rittmann, B.E., 1983. Secondary utilization of trace organics by biofilms on porous media. J. Am. Water Works Assoc. 75 (9), 463–469.
Terry, L.G., Summers, R.S., 2018. Biodegradable organic matter and rapid-rate biofilter performance: a review. Water Res. 128, 234–245.
Torång, L., Nyholm, N., Albrechtsen, H.J., 2003. Shifts in biodegradation kinetics of the herbicides MCPP and 2,4-D at low concentrations in aerobic aquifer materials. Environ. Sci. Technol. 37 (14), 3095–3103.
Trautwein, C., Kümmerer, K., 2011. Incomplete aerobic degradation of the antidiabetic drug metformin and identification of the bacterial dead-end transformation product guanylurea. Chemosphere 85 (5), 765–773.
Trejo-Castillo, R., El Kassis, E.G., Cuervo-López, F., Texier, A.C., 2021. Cometabolic biotransformation of benzotriazole in nitrifying batch cultures. Chemosphere 270, 129461.
Vandermaesen, J., Horemans, B., Degryse, J., Boonen, J., Walravens, E., Springael, D., 2016. Mineralization of the common groundwater pollutant 2,6-dichlorobenzamide (BAM) and its metabolite 2,6-dichlorobenzoic acid (2,6-DCBA) in sand filter units of drinking water treatment plants. Environ. Sci. Technol. 50 (18), 10114–10122.
Wang, J., de Ridder, D., van der Wal, A., Sutton, N.B., 2021. Harnessing biodegradation potential of rapid sand filtration for organic micropollutant removal from drinking water: a Review. Crit. Rev. Environ. Sci. Technol. 51 (18), 2086–2118.
Wang, J., Zhang, C., Poursat, B.A.J., de Ridder, D., Smidt, H., van der Wal, A., Sutton, N. B., 2022. Unravelling the contribution of nitrifying and methanotrophic bacteria to micropollutant co-metabolism in rapid sand filters. J. Hazard. Mater. 424 D, 127760.
Westerhoff, P., Yoon, Y., Snyder, S., Wert, E., 2005. Fate of endocrine-disruptor, pharmaceutical, and personal care product chemicals during simulated drinking water treatment processes. Environ. Sci. Technol. 39 (17), 6649–6663.
Yang, W., Zhou, H., Cicek, N., 2014. Treatment of organic micropollutants in water and wastewater by UV-based processes: a literature review. Crit. Rev. Environ. Sci. Technol. 44 (13), 1443–1476.
Zearley, T.L., Summers, R.S., 2012. Removal of trace organic micropollutants by drinking water biological filters. Environ. Sci. Technol. 46 (17), 9412–9419.
Zhou, J., Wang, D., Ju, F., Hu, W., Liang, J., Bai, Y., Liu, H., Qu, J., 2022. Profiling microbial removal of micropollutants in sand filters: biotransformation pathways and associated bacteria. J. Hazard. Mater. 423 B, 127167.